Insect Biochemistry and Molecular Biology 134 (2021) 103583

Contents lists available at ScienceDirect

Insect Biochemistry and Molecular Biology

journal homepage: www.elsevier.com/locate/ibmb

Interacting C/EBPg and YBP regulate DNA methyltransferase 1 expression in *Bombyx mori* embryos and ovaries

Hao Lyu [a,b], Guanfeng Xu [a,b], Xuezhen Peng [a,b], Chengcheng Gong [a,b], Yuling Peng [a,b], Qisheng Song [c], Qili Feng [a,b], Sichun Zheng [a,b,*]

[a] Guangdong Provincial Key Laboratory of Insect Developmental Biology and Applied Technology, Institute of Insect Science and Technology, School of Life Sciences, South China Normal University, Guangzhou, 510631, China

[b] Guangzhou Key Laboratory of Insect Development Regulation and Applied Research, Institute of Insect Science and Technology, School of Life Sciences, South China Normal University, Guangzhou, 510631, China

[c] Division of Plant Sciences, College of Agriculture, Food and Natural Resources, University of Missouri, Columbia, MO, 65211, USA

ARTICLE INFO

Keywords:
DNA methylation
DNA methyltransferase
Transcription regulation
Reproduction
Bombyx mori

ABSTRACT

DNA methylation is an important epigenetic modification. DNA methyltransferases (Dnmts), which catalyze the formation of 5-methylcytosine, play a role in ovarian and embryonic development in some insects. However, the underlying mechanism of Dnmt in mediating ovarian and embryonic development remains unclear. In this study, the regulation and function of *Bombyx mori Dnmt1* were investigated. By progressively deleting the sequence upstream of *Dnmt1*, a region located between −580 and −560 region from the transcription initiation site was found to have the most transcriptional activity. Electrophoretic mobility shift assay and chromatin immunoprecipitation demonstrated that transcription factor Y box binding protein (YBP), a homolog of human Y box binding protein 1 (YBX1), bound to the −580 to −560 region. YBP knockdown and overexpression in a *Bombyx* cell line indicated that YBP activates *Dnmt1* expression. Furthermore, GST-pulldown and co-immunoprecipitation demonstrated that YBP and ovarian CCAAT/enhancer binding protein (C/EBPg) could bind each other. Simultaneous knockdown of *C/EBPg* and *YBP* was more effective than single-gene RNAi in inhibiting *Dnmt1* expression and reducing the hatching rate. These results demonstrated that the interaction of C/EBPg and YBP activated *Dnmt1* expression. Correlated with the expression profiles of the studies genes, our results suggest that high-level expression and interaction of C/EBPg and YBP in ovaries and embryos enhance the expression of *Dnmt1*, thus ensuring high reproduction rate in *B. mori*.

1. Introduction

DNA methylation is an important epigenetic modification. DNA methyltransferase (Dnmt) catalyzes the formation of 5-methylcytosine (5 mC), in which the methyl group is transferred to the fifth carbon of the pyrimidine ring of cytosine. In animals, 5mCs are mainly located in the cytosine of dinucleotide CG (or CpG), in addition to a small proportion of CHG or CHH (H represents A, G, or T) (Feng et al., 2010). There are three types of DNA methyltransferases in animals. Dnmt1 is a maintenance Dnmt that replicates the methylation pattern from the template strand to the newly synthesized strand in DNA replication; Dnmt3 is a de novo methyltransferase that targets unmethylated cytosine to generate new 5 mC (Bird, 2002), while Dnmt2 can mediate RNA methylation compared to other members of the Dnmt family (Goll et al., 2006). In general, DNA methylation plays a role in transcriptional silencing in mammals in response to intrinsic or extrinsic signals. DNA methylation is deposited at a silent locus, maintaining its metaplastic state, thereby locking transcriptional inactivation (Cedar and Bergman, 2009; Jaenisch and Bird, 2003). DNA methylation is involved in a variety of functions, such as X-chromosome inactivation, genomic

Abbreviations: C/EBPg, CCAAT/enhancer binding protein; Dnmt1, DNA methyltransferase 1; FBS, fetal bovine serum; TBST, Tris buffered saline tween; DTT, dithiothreitol; SDS, sodium dodecyl sulfate; RNAi, RNA interference; HEPES, 4-(2-Hydroxyethyl)piperazine-1-ethanesulfonic acid; PMS, phenylmethyl sulfonyl-fluoride; ORF, open reading frame; P, phosphate buffer saline; YBP, ybox binding protein.

* Corresponding author. Guangdong Provincial Key Laboratory of Insect Developmental Biology and Applied Technology, Institute of Insect Science and Technology, School of Life Sciences, South China Normal University, Guangzhou, 510631, China.

E-mail address: sczheng@scnu.edu.cn (S. Zheng).

https://doi.org/10.1016/j.ibmb.2021.103583
Received 12 November 2020; Received in revised form 5 April 2021; Accepted 20 April 2021
Available online 16 May 2021
0965-1748/© 2021 Elsevier Ltd. All rights reserved.

imprinting, transposable element inhibition, and genome-wide silencing of developmental loci (Bonasio et al., 2010; Cedar and Bergman, 2009; Hackett et al., 2012).

In insects, the DNA methylation rate is much lower than that of mammals and plants. For example, DNA methylation rates of *Apis mellifera* and *Camponotus floridanus* are less than 1% and 0.2%, respectively (Yan et al., 2015), and the methylation rate in the silk gland of *Bombyx mori* is 0.15%–0.19% (Xiang et al., 2010). Despite the low methylation rate, DNA methylation plays a role in insect development. Genome bioinformatics analysis showed that different methylation rates affected wing differentiation in *Sogatella furcifera* (Zhou et al., 2013) and caste differentiation in *A. mellifera* (Shao et al., 2014). DNA methylation inhibitor (5-aza-dC) treatment resulted in the wing deformity of *B. mori* through the upregulation of transcription factor ara-mediated chitinase (Xu et al., 2020). *Dnmt1* RNAi results showed that de-methylation significantly decreased oviposition or egg hatch rates in *B. mori* (Xiang et al., 2010) and *Oncopeltus fasciatus* (Bewick et al., 2019), and resulted in abnormal embryos of *Blattella germanica* (Ventos-Alfonso et al., 2020). These results suggest that DNA methylation plays an important role in the reproduction of holometabolous and hemimetabolous insects.

Bioinformatics analysis of genomes has revealed that Dnmt1, Dnmt2, and Dnmt3 exist in insects as in mammals (Yan et al., 2015). However, not all insects have both Dnmt1and Dnmt3 for DNA methylation. For example, neither Dnmt1 nor Dnmt3 was found in *Drosophila melanogaster* (Lyko and Maleszka, 2011), and only Dnmt1 was found in *B. mori* (Yan et al., 2015). The activity of *B. mori* Dnmt1 was demonstrated (Xu et al., 2018), but whether *B. mori* Dnmt1 has the Dnmt3 function as in other animals is unclear (Mitsudome et al., 2015). Since de novo methylation activity may be functioning in early embryos, the role of Dnmt1 in early embryos, ovaries, and cultured cells may be different. However, the result of *Dnmt1* RNAi showed that *Dnmt1* is important for *B. mori* embryonic development (Xiang et al., 2010). The tissue expression levels of Dnmts have been reported in multiple insects, in which Dnmt expression levels in the ovary and embryo are higher than those in the testis (Kay et al., 2018; Robinson et al., 2016; Yang et al., 2014; Zhang et al., 2015; Zwier et al., 2012). These results suggest that the higher expression levels of Dnmts may be the reason for their influence on ovarian and embryonic development. However, the regulatory mechanism of *Dnmts* in the ovary and the embryo is unclear.

In this study, the regulatory mechanism of *Dnmt1* expression in the ovary and the embryo of *B. mori*, a model insect of Lepidoptera, was investigated, and its role in embryonic development was confirmed. We found that the interaction of transcription factors, Y box-binding protein (YBP) and CCAAT/enhancer-binding protein (C/EBPg), activates *Dnmt1* expression, which in turn regulates ovarian and embryonic development.

2. Materials and methods

2.1. Insect and cell line

The *B. mori* multivoltine strain of p50 was obtained from the Research and Development Center of the Sericultural Research Institute, the Academy of Agricultural Sciences of Guangdong Province, China. Larvae were reared on fresh mulberry leaves at 25 °C and a photoperiod of 12 h light:12 h darkness.

The *B. mori* DZNU-Bm-12 (Bm12) cell line was originally developed from ovarian tissues (Khurad et al., 2009). The cells were maintained at 28 °C in Grace medium (Invitrogen, New York, USA) containing 10% FBS (Gibco, New York, USA) and subcultured at a ratio of 1:3 every 4 days.

2.2. DNA-protein pull-down assay

Single-stranded probes of the wild type and mutant promoter fragments of *B. mori Dnmt1* were heated at 95 °C for 10 min and then slowly cooled to room temperature to obtain the double-stranded probes. To minimize non-specific interactions, the oligo-bead complexes were incubated for 30 min with a blocking buffer, containing 0.25% bovine serum albumin (BSA), 10 mM HEPES, 10 mM glutamate potassium, 2.5 mM DTT, 10 mM magnesium acetate, 5 mM EGTA, 3.5% glycerine, 0.003% NP-40 and 0.5% PVP-K30. Immobilized double-stranded probes were incubated with 20 μg of nuclear extract for 4 h at 4 °C with constant rotation in 400 μL of protein binding buffer (10 mM HEPES, 100 mM glutamate potassium, 80 mM KCl, 2.5 mM DTT, 10 mM magnesium acetate, 5 mM EGTA, 3.5% glycerine and 0.001% NP-40). Protein-DNA complexes were then washed for three times with wash buffer (10 mM HEPES, 100 mM glutamate potassium, 2.5 mM DTT, 10 mM magnesium acetate, 5 mM EGTA, 3.5% glycerine, 0.05% BSA, 0.05% NP-40). Proteins bound with the probe were eluted with 20 μL of denaturing Laemmli sample loading buffer (50 mM Tris-HCl, 100 mM DTT, 2% SDS, 0.1% bromophenol blue and 10% glycerine) at 37 °C for 15 min, and were used for SDS-PAGE. A single differential band between the wild-type probe and the mutant probe was isolated from the gel of SDS-PAGE and sent to the company (Fitgene, Guangzhou, China) for LC-MS/MS analysis.

2.3. Nuclear protein preparation and electrophoretic mobility shift assay (EMSA)

Tissues or cells were harvested and washed once with 10 mM PBS (pH = 7.4). Cell nuclear proteins were extracted using NE-PER Nuclear and Cytoplasmic Extraction Reagents (Thermo Scientific, Waltham, USA) following the manufacturer's protocol. Protein concentrations in nuclear extracts were determined using a BCA Protein Assay Reagent Kit (Thermo Scientific).

EMSA was conducted using a LightShift Chemiluminescent EMSA Kit (Thermo Scientific) following the manufacturer's protocol. Oligonucleotides conjugated with biotin at the 5′ end of probes were synthesized by Invitrogen (Invitrogen, New York, USA). Oligonucleotide probes were heated at 95 °C for 10 min and then slowly cooled to room temperature. The 4 μg nuclear protein or 2 μg purified C/EBPg proteins were incubated for 20 min at room temperature with a 20 μL binding buffer containing 50 ng poly (dI-dC), 2.5% glycerol, 0.05% nonidet P 40, 50 mM KCl, 5 mM $MgCl_2$, 4 mM EDTA, and 20 nmol of a biotinylated end-labeled double-stranded probe. Different concentrations of cold probes (unlabeled) were added to the binding mixture as competitors. Polyacrylamide gels (6%) were run at 100 V for 1.5 h on ice. After electrophoresis, proteins were blotted onto positively charged Hybond N+ nylon membranes (GE Healthcare, USA). The membranes were visualized using Chemiluminescent Nucleic Acid Detection Module (Thermo Scientific) and exposed using ChemiDoc™ Touch Imaging System (Bio-rad, California, USA).

2.4. RNA isolation and quantitative real-time PCR (qRT-PCR)

Total RNA was extracted from cell samples using Trizol reagent (TaKaRa, Dalian, CN). cDNAs were synthesized using a First Strand cDNA Synthesis Kit (TaKaRa) following the manufacturer's protocol. qPCR analysis was performed using 2x Eastep® qPCR Master Mix (Promega, Wisconsin, USA). The relative mRNA levels were normalized to the expression level of the house-keeping gene, *ribosomal protein 49* (*Rp49*) (GenBank accession No: AB048205) (Kostal et al., 2009) and *18S ribosomal RNA* gene (18S rRNA) (NCBI accession No: DQ347470.1), and analyzed using the $2^{-\triangle\triangle Ct}$ method (Livak and Schmittgen, 2001). All data included three biological replicates.

2.5. Transient transfection, promoter activity assay, RNAi and overexpression of genes

The Bm12 cells in the logarithmic growth phase were inoculated in culture media in 24-well culture plates (Corning, New York, USA) and

cultured for 12 h. Cell transfection and co-transfection were conducted when cells were in about 80% confluence. A 1500 bp fragment of *Dnmt1* promoter and its truncated fragments were cloned and ligated to the luciferase reporter vector (pGL3). A mixture containing 0.5 μg of the pGL3-derived reporter plasmid DNA, 50 ng of the internal control plasmid (*pRL-SV40*), and 3 μL of the Fugene HD transfection reagent (Promega, Wisconsin, USA) in Opti-MEM Reduced Serum Medium (Life Technologies, California, USA) was added to Bm12 cells in Grace medium. Cells were cultured for 48 h at 28 °C, washed for twice with filtered PBS and lysed in 100 μL Passive Lysis Buffer (Promega). Samples were centrifuged at 800 g for 5 min at room temperature. The resulting supernatant was used to analyze luciferase activity with a GLOMAX MULTI JR detection system (Promega) following the manufacturer's protocol. Luciferase activity was normalized to the Renilla luciferase activity of *pRL-SV40*. For YBP or C/EBPg overexpression, *YBP* or *C/EBPg* ORF was constructed into the vector, *pEGFP-N1*, to generate the vector, *pYBP-EGFP* or *pC/EBPg-EGFP*. These two vectors were transfected or co-transfected with the pGL3-derived reporter plasmid DNA to determine gene expression. For *YBP* or *C/EBPg* RNAi, double-stranded RNAs (dsRNA) of both genes were synthesized with the T7 RiboMAX™ Express RNAi System (Promega) following the manufacturer's instructions. *GFP* dsRNA was used as a control. Two micrograms of dsRNA were transfected or co-transfected with the pGL3-derived reporter plasmid DNA to determine gene expression. All assays were repeated with three generations of cells. Specific PCR primers for dsRNA synthesis are listed in Table S1.

2.6. Chromatin immunoprecipitation (ChIP)

ChIP was performed in the *Bm*12 cells following the instruction of Pierce Magnetic ChIP Kit (Thermo Scientific). Briefly, approximately 4 $\times$ 10^6 cells were set up, cross-linked with 1% formaldehyde for 10 min, and then de-cross-linked with glycine. The cells were treated with MNase diluted in MNase Digestion Buffer for 15 min at 37 °C, and then nuclei were released from cells using ultrasonic breaking with several pulses and 20 s ice-cold interval. The protein-DNA complexes were immunoprecipitated using specific antibody, enriched by Magnetic Beads, and cross-linked reversely at 65 °C for 30 min with vigorous rotation. DNA was purified using the column method (Thermo Scientific), and detected by qPCR. Input (10%) was used as a control.

2.7. Antibody preparation

YBP recombinant proteins were obtained using the prokaryotic expression system with the pGEX-6p1 vector. The blank serum of five-week-old BALB/c strain mice was collected as a negative control, and stored at −80 °C. One week later, Freund's complete adjuvant and purified proteins were mixed at a ratio of 1:1, and shaken for more than 4 h to emulsify the protein completely. The emulsified proteins were injected into the mouse subcutis for immunization. Three injections of the proteins emulsified with 1:1 Freund's incomplete adjuvant were performed in the following 3 weeks. The mouse blood was collected, incubated for 1 h at 37 °C, and then overnight at 4 °C. The next day, the blood was centrifuged at 12000 rpm for 10 min. The supernatant was saved at −80 °C for later use.

2.8. Western blot analysis

Protein analysis was performed using SDS-PAGE gel and Western blot. A total of 40 μg proteins extracted from tissues or *Bm*12 cells were denatured and then separated in 12% SDS-PAGE gel, followed by transferring to a nitrocellulose blotting membrane (GE healthcare, Chicago, USA). The membrane was blocked with Tris-buffered saline with Tween-20 (TBST) (20 mM Tris-HCl, 150 mM NaCl, 0.05% Tween-20, pH7.4) containing 3% (w/v) BSA for 2 h at room temperature, followed by hybridization overnight at 4 °C in TBST containing 1% BSA and primary antibody. The secondary antibody was a horseradish peroxidase (HRP)-conjugated antibody (Dingguo Biotechnology, Beijing, China). Primary and secondary antibodies were diluted 1:1000 and 1:10000 in TBST with 1% (w/v) BSA, respectively. Anti-tubulin antibody (Dingguo Biotechnology) was used to show equal loading of proteins on gels.

2.9. Co-immunoprecipitation (Co-ip)

Bm12 cells were plated in 12-well plates and transiently transfected with HD2000 Transfection Reagent (Promega) following the manufacturer's instructions. Cells were transfected with 2 μg of the C/EBPg-EGFP recombinant vector plasmids. At 48 h post-transfection, the cells were lysed using 200 μL per well of cell lysis buffer for Western blot and Co-ip (Beyotime, Shanghai, China) containing a final concentration of 1 mM PMSF. The suspension was transferred to a 1.5 mL EP tube, and centrifuged at 4 °C and 12,000 rpm for 5 min. The resulting supernatant was transferred to a new tube, leaving 20 μL as an input. A total of 70 μL of anti-GFP agarose beads with GFP antibody (KTSM1301, Alpa-life, Shenzhen, China) were prepared for each sample, and washed for twice with PBS. About 300 μL of the previously collected proteins were added to each sample, and slowly shaken at 4 °C for 4–6 h or overnight. After the incubation was completed, the sample was centrifuged at 4 °C for 30 s, and the supernatant was removed. The pre-cooled PBS (800 μL) was added to the pellet, and washed for three times. Each sample was dissolved with 20 μL of PBS and 5 μL of 5 x protein loading buffer, and boiled for 10 min to denature protein before SDS-PAGE and Western blot.

2.10. GST pull-down

The ORFs of *YBP* and *C/EBPg* were constructed into the pGEX-6p1 vector as bait protein. About 50–70 μL GST-Beads (immobilized glutathione) were added into an EP tube, rinsed once with 800 μL PBS containing 1% Triton-100, and then mixed with the YBP proteins expressed in prokaryotic system for 1 h. Samples were washed for three times with PBS and 1% Triton-100 and three times with PBS. A total of 20 μL (PBS and beads) was saved as Offer. The ORF end of *YBP* was tagged with the flag protein and constructed into pEGFP-N1 without GFP fragment. After being transfected into Bm12 cells for 48 h, it was enriched as pull-down incubated proteins. After removing culture medium, cells were washed once with PBS, added with 300 μL of lysate, and leaved at 4 °C for 30 min. Cells were then collected, sonicated and centrifuged. About 20 μL was reserved for the offer, the remaining samples were mixed with bait protein and GST-Beads, added with PBS to 600 μL volume, and incubated overnight at 4 °C. Samples were washed for three times with PBS containing 1% Triton-100, and then washed for three times with PBS. Western blot method was used to detect the presence of incubated proteins.

2.11. Effect of dsRNA injection on the egg hatch rate

Double-stranded RNA was injected into fertilized eggs within 5 h after egg laying through a microinjection system (Eppendorf, Hamburg, GER). A double-needle microinjection system was used. Briefly, a small hole in an egg was made using a very small steel needle, then the dsRNA was injected through a capillary glass needle, and finally a small amount of glue was applied to the injection port to prevent the outflow of the fluid in the egg. At 24 h after injection, portion of fertilized eggs were used to extract total RNA for detecting the mRNA expression level of corresponding genes by qPCR. About 7 days later, the hatch rate of eggs was calculated. For each injection, each group of eggs were evenly arranged in 9 rows x 12 columns on a slide, 324 eggs on three slides were injected. Three biological repeats were performed.

2.12. Statistical analysis

Data are presented as mean ± SEM. Significance for the purpose of group comparisons were calculated using student's *t*-test (*p < 0.05, **p < 0.01, ***p < 0.001).

3. Results

3.1. Dnmt1 RNAi decreases the egg hatch rate

Dnmt1 plays a role in *B. mori* embryonic development (Xiang et al., 2013). To confirm this result, *Dnmt1* RNAi was performed. The qPCR result showed that *Dnmt1* was expressed during early stages of embryonic development in wild-type *B. mori* (Fig. 1A). After *Dnmt1* dsRNA was injected into the newly fertilized egg, the hatch rate was determined 7 days later. The fertilized eggs started to hatch at 7.5 days post-fertilization in the control group, and reached a 33.07% hatch rate at day 10, while only a 2.68% hatch rate was observed at day 10 in the *Dnmt1* RNAi group (Fig. 1B). These results indicate that *Dnmt1* is expressed in the early developmental stages and affects the egg hatch rate.

YBP enhances *Dnmt1* expression by directly binding to the −580 to −560 enhancer in the *Dnmt1* promoter.

After demonstrating that *Dnmt1* is involved in the regulation of embryonic development, we studied how *Dnmt1* is activated to play a role in this development process. To elucidate the regulatory mechanism of *Dnmt1* expression, a 1500 bp fragment of the *Dnmt1* promoter was cloned, and the activities of stepwise truncated fragments of the promoter were determined. For the determination of the luciferase activity, the enhancer fragments with the core promoter fragment of *Dnmt1* were individually ligated into vector pGL3. At first, the 1500-bp promoter fragment was truncated into 1000 and 500 bp fragments. The result showed that the −1000 to −500 region from the transcription initiation site (+1), which is the first base of *Dnmt1* mRNA, had higher activity (Fig. 2A). Then, higher activity of the −680 to −500 region inside of the −1000 to −500 region was identified (Fig. 2B). Furthermore, the −600 to −520 region was confirmed to be the most active region in the −680 to −500 region (Fig. 2C). To determine the regulatory region, the −600 to −520 region was further truncated, and the −600 to −560 region was identified to have higher activity (Fig. 2D). To further confirm the activity of the −600 to −560 region, the luciferase activity of the −600 to −560 region with mutated nucleotides at −600 to −580 region or −580 to −560 region was determined. The result showed the activity of the −600 to −560 region was significantly decreased by the mutation at −580 to −560 region (Fig. 2E and F). These results demonstrated that the −580 to −560 region of the promoter had the greatest effect on *Dnmt1* transcription.

To identify the nuclear proteins that may bind to the −580 to −560 region of the promoter, a DNA pull-down experiment was conducted. The fragment of the −580 to −560 region was labeled with biotin and then linked to streptavidin-coated beads. The complex was then incubated with the nuclear proteins isolated from Bm12 cells. The proteins that bound to the biotin-labeled probes were separated on a SDS-PAGE gel, and the differentiated protein bands were excised and subjected to LC-MS/MS analysis. The result showed that there was one differentiated protein band between the wild-type probe and the mutated probe used. The size of the protein band was approximately 30 kDa (Fig. S1). LC-MS/MS analysis presented six putative transcription factors (Table S2), and their predictive scores were 10154 (Y-box protein, YBP), 1272 (chromobox protein homolog 5-like, CBX5), 875 (Exuperantia, EXU), 751 (Interleukin enhancer-binding factor isoform 1, IEF), 662 (DnaJ-10, DnaJ), and 437 (DNA supercoiling factor, SCF). YBP had a much higher predictive score than other genes, suggesting that YBP may bind to the enhancer in the *Dnmt1* promoter. We further selected the three transcription factors with higher predictive score besides YBP to analyze their relationship with *Dnmt1*. The *dscbx5*, *dsExu*, and *dsief* were transfected into Bm12 cells for 24 h, and *Dnmt1* and their mRNA levels were determined. Knock down of these three transcription factors (Fig. S2A) had no influence on the expression level of *Dnmt1* (Fig. S2B). However, the *YBP* (Fig. 3A) and *Dnmt1* (Fig. 3B) mRNA levels were significantly decreased after the *YBP* dsRNA was transfected into Bm12 cells for 24 and 48 h. This indicated that YBP regulates the *Dnmt1* expression. Therefore, a binding assay of YBP (GenBank accession no.: BAF45318) to the −580 to −560 region of the promoter was performed. The recombinant YBP protein was obtained using prokaryotic expression system. EMSA with YBP pure proteins showed that the recombinant YBP specifically bound to the biotin-labeled probe (−580 to −560 region) (Fig. 3C, lanes 2 and 3), and this band could be competed off by the unlabeled probe (cold probe) (Fig. 3C, lanes 5 and 6) but not by the mutated probe (Fig. 3C, lane 4), suggesting that YBP specifically binds to the enhancer in the *Dnmt1* promoter.

EMSA with nuclear proteins from YBP-GFP-overexpressed Bm12 cells showed that there were nuclear proteins binding to the labeled probe (Fig. 3D, lane 2), and this binding could be competed off by unlabeled cold probe (Fig. 3D, lanes 3 and 4). However, no nuclear proteins could bind to the labeled mutated probe (Fig. 3D, lane 5). When the antibody and nuclear proteins were added before the probe, there was no strong binding band detected (Fig. 3D, lane 7), presumably due to the blockage of protein access to probe by the antibody. The strong band was supershifted when nuclear protein and the probe were mixed before the addition of the GFP antibody (Fig. 3D, lane 8), which was against the GFP tag of YBP-GFP proteins in Bm12 cells.

In addition, ChIP was performed to confirm the EMSA results. YBP-flag vector was transfected into Bm12 cells, and the cell protein was prepared. The qPCR result showed that the PCR product in the YBP-flag-transfected sample with flag antibody was much higher than that with control IgG antibody, and sequence analysis demonstrated that the PCR product with the YBP-flag-transfected sample was the fragment of the

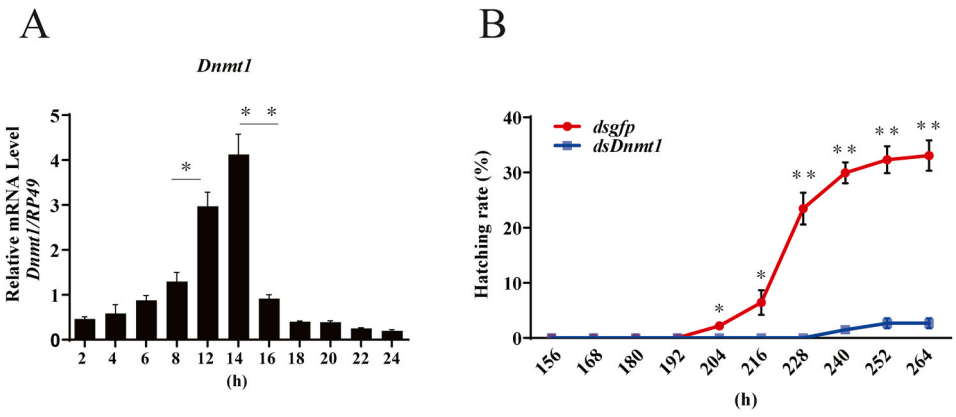

Fig. 1. The expression profile of DNA methyltransferase 1 (*Dnmt1*) in fertilized eggs and its effect on the hatch rate of fertilized eggs. (A) *Dnmt1* expression profile at the first day of wild-type *B. mori* embryonic development. (B) Difference in the hatch rate after injection of *dsDnmt1*. The relative mRNA level of *Dnmt1* was normalized to the expression level of *ribosomal protein 49* (*RP49*). D: Day. Each data point is mean ± SEM of three independent assays. For the *t*-test: *p < 0.05, **p < 0.01, ***p < 0.001.

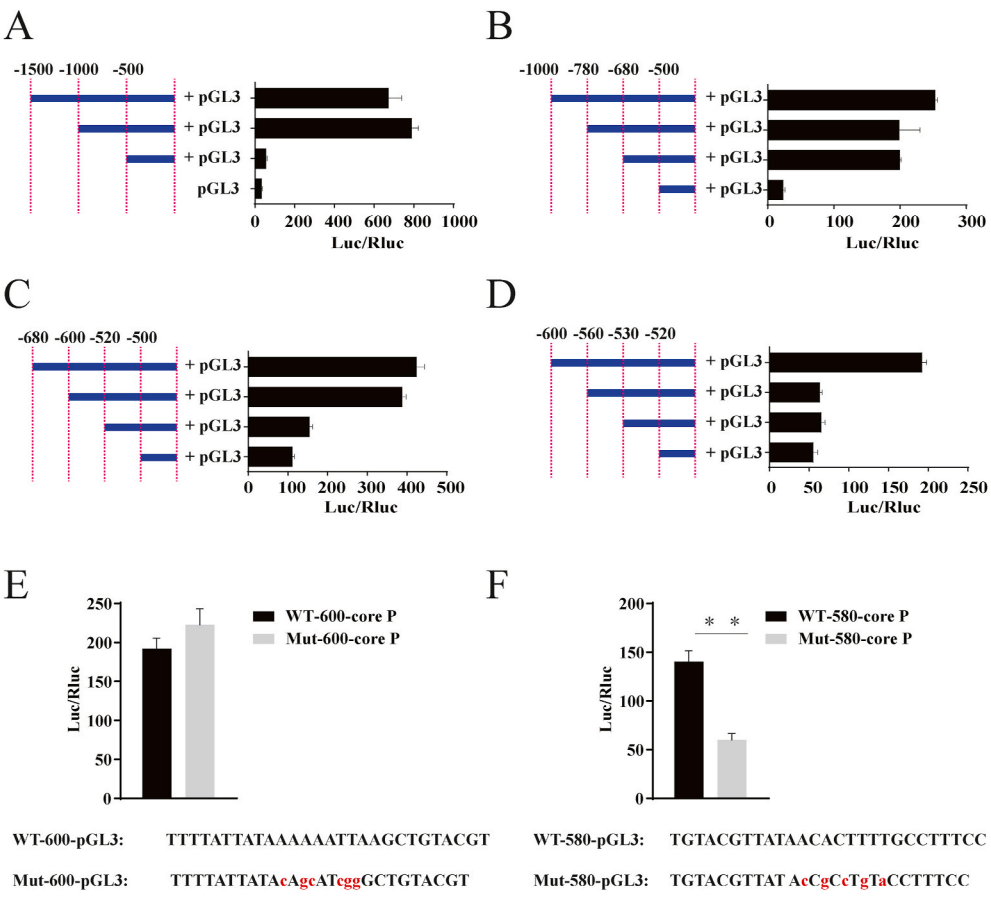

Fig. 2. The −580 to −560 enhancer in the promoter enhances the *Dnmt1* transcription. (AtoD) Luciferase activities of the truncated regions from −1500 to −500 upstream transcription start site in Bm12 cells. (E) The luciferase activity detection of the −600 to −580 region and the mutant region. WT-600-pGL3: The −600 to −580 region of the *Dnmt1* promoter was constructed into pGL3 vector. Mut-600-pGL3: The mutant DNA sequence of the −600 to −580 region was constructed into pGL3 vector. (F) The luciferase activity determination of the −580 to −560 region and its mutant fragments. Each data point is the mean ± SEM of three independent assays. For the *t*-test: *p < 0.05, **p < 0.01, ***p < 0.001.

−580 to −560 region (Fig. 3E). These data confirmed that YBP binds to the −580 to −560 region.

To determine whether YBP activates the *Dnmt1* expression by binding to the enhancer in the *Dnmt1* promoter, YBP-EGFP vector and the −580 to −560 region-included pGL3 vector were co-transfected into Bm12 cells, and the reporter activity was quantified at 48 h post-transfection. The result showed that YBP overexpression significantly enhanced the activity of the −580- to −560-bp region but not the mutated region compared to GFP overexpression (Fig. 3F). On the contrary, *YBP* RNAi inhibited the activity of the −580- to −560-bp region compared to *gfp* RNAi (Fig. 3G). All of the data indicate that YBP enhances the *Dnmt1* expression by directly binding to the enhancer in the *Dnmt1* promoter.

3.2. The interaction of C/EBPg and YBP promotes the Dnmt1 expression

In human cells, the interaction of Y-box and acetylated endonuclease APE1 activates gene expression (Sengupta et al., 2011). Does YBP also need a cofactor to activate the *dnmt1* expression? Since insect Dnmt1 is highly expressed in ovaries (Kay et al., 2018; Robinson et al., 2016), we assumed that there might be an ovary-specific transcription factor enhancing the binding of YBP to the enhancer in the *Dnmt1* promoter. Therefore, we searched for ovary-specific transcription factors in the silkworm genome, and a gene, C/EBPg (Sourmeli et al., 2005), was found and selected to test its interaction with YBP. C/EBPg-GFP overexpression demonstrated that C/EBPg enhanced the activity of the −580- to −560-bp region but not the mutated one in Bm12 cells compared to GFP overexpression (Fig. 4A). Furthermore, we investigated whether both proteins form a complex to activate *Dnmt1* expression using GST pull-down and immunocoprecipitation (Co-ip). In GST pull-down experiments, GST-tagged C/EBPg proteins obtained from the prokaryotic expression system were linked to GST agarose gel beads and incubated with YBP-flag proteins obtained from YBP-flag-overexpressed Bm12 cells. Western blot was then performed to determine the interaction between both proteins with flag antibody. The result showed a band in the C/EBPg-GST and YBP-flag pull-down sample compared to the GST and YBP-flag sample (Fig. 4B). Similarly, a band appeared in the GST-tagged YBP and C/EBPg-flag proteins compared to the GST and C/EBPg-flag protein (Fig. 4C), suggesting the interaction between YBP and C/EBPg proteins. In the Co-ip experiment, C/EBPg-GFP proteins were used as the bait protein, YBP proteins in the cell proteins were captured by C/EBPg-GFP and recognized by YBP antibody, but YBP could not be coprecipitated by GFP proteins used as the bait protein and recognized by YBP antibody (Fig. 4D). The Co-ip results are consistent with the previous GST pull-down results (Fig. 4B and C). The above result confirmed that C/EBPg and YBP can bind each other.

To investigate whether the complex of C/EBPg and YBP enhances *Dnmt1* expression, *Dnmt1* transcriptional activity was determined. The result showed that co-overexpression of both C/EBPg and YBP proteins produced an additive stimulatory effect to enhance the *Dnmt1* transcription compared to C/EBPg or YBP overexpression alone (Fig. 4E). In contrast, the mRNA level of *Dnmt1* was significantly inhibited by the combined transfection of *ybp* and *C/EBPg* dsRNA in Bm12 cells compared to that transfected only with *ybp* or *C/EBPg* dsRNA (Fig. 4F). Taken together, these results indicate that both C/EBPg and YBP collaborate to upregulate the *Dnmt1* transcription by forming a complex in the enhancer.

C/EBPg and YBP participate in the embryonic development by coordinated regulation of *Dnmt1* expression.

The above data showed that C/EBPg and YBP directly bound to the −580 to −560 region of the *Dnmt1* promoter to regulate the expression

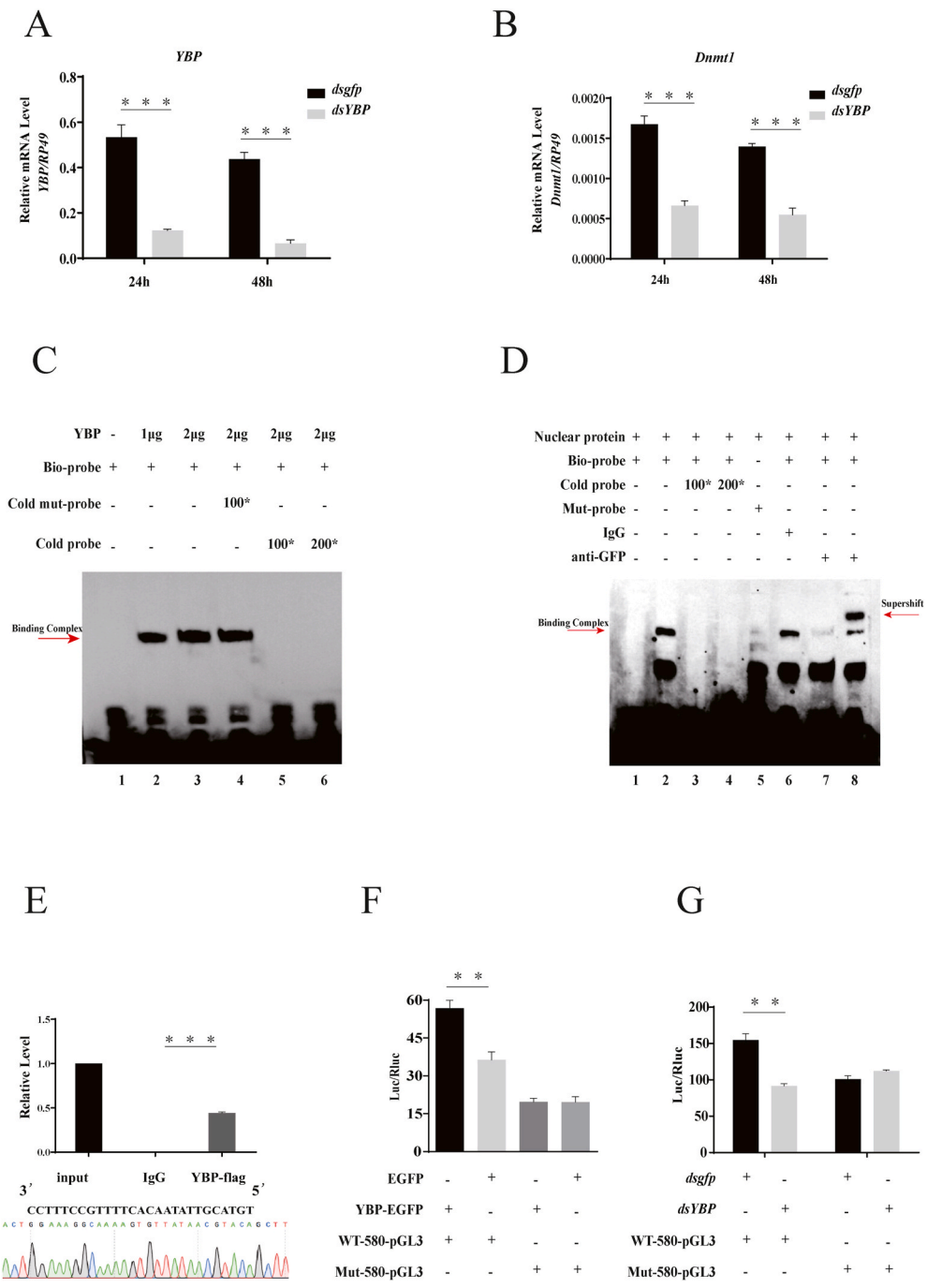

Fig. 3. Y box binding protein (YBP) enhances the *Dnmt1* expression by directly binding to the −580 to −560 region of the *Dnmt1* promoter. (A) Electrophoretic mobility shift assay (EMSA) of YBP pure proteins to the biotin-labeled probe of the −580 to −560 region. (B) EMSA of nuclear proteins from YBP-EGFP-overexpressed Bm12 cells, and supershift was analyzed using EGFP antibody. The penultimate lane: the protein was incubated with the antibody for 1 h, then the probe was added and incubated for 1 h. The last lane: the protein is incubated with the probe for 1 h before adding the antibody for 1 h. (C) Immunoprecipitation analysis of the binding of YBP-flag overexpressed in Bm12 cells with the −580 to −560 region of the *Dnmt1* promoter, recognized by flag antibodies. Immunoprecipitation enriched DNA fragments were analyzed by qPCR. Samples was normalized using DNA present in the 10% input material. The sequence above the bar graph is the sanger sequencing result of the PCR product amplified by using the ChIP product as a template. (D) The effect of YBP overexpression on the luciferase activity of the −580 to −560 region, and EGFP was used as a control. (E) The effect of *YBP* RNAi on the luciferase activity of the −580 to −560 region, and *dsgfp* was used as a control. (F to G) After transfection of *YBP* dsRNA in Bm12 cells, the mRNA levels of *YBP* (F) and *Dnmt1* (G) were detected. The relative mRNA level of *Dnmt1* was normalized to the expression level of *RP49*. Each data point is the mean ± SEM of three independent assays. For the *t*-test: *p < 0.05, **p < 0.01, ***p < 0.001.

of *Dnmt1*. Do C/EBPg and YBP regulate the hatch rate like *Dnmt1*? The expression pattern analysis showed that *YBP* was upregulated at 8–14 h after fertilization (Fig. 5A) like *Dnmt1* (Fig. 1A), and *C/EBPg* was expressed almost throughout the entire first day (Fig. 5B). The dsRNA of *C/EBPg* or *YBP* was injected into the silkworm fertilized egg within 2 h of fertilization. Then, qPCR analysis demonstrated that the mRNA level of *C/EBPg* or *YBP* was significantly reduced by the dsRNA injection 24 h post-injection (Fig. 5C), and the mRNA level of *Dnmt1* was also significantly reduced by *C/EBPg*, *YBP*, or *Dnmt1* RNAi (Fig. 5D). RNAi knockdown of *C/EBPg* or *YBP* significantly reduced the hatch rate, but the effectiveness of *C/EBPg* or *YBP* was lower than *Dnmt1* RNAi. However, when *C/EBPg* and *YBP* dsRNAs were simultaneously injected into fertilized eggs, the hatch rate was significantly decreased and lower than *C/EBPg* or *YBP* RNAi (Fig. 5E). The appearance of the fertilized egg injected with *dsDnmt1*, *dsC/EBPg,* or *dsYBP* was not different than the control (*dsgfp*) until the head pigmentation stage (180 h after egg deposition). At this stage, the chitinous shell of the normal larval head began to blacken, while the *dsDnmt1*, *dsC/EBPg,* or *dsYBP*-injected larvae did not. Inside these gene-knocked down eggs, the larval bodies were rotting, the development of the epidermis and head shell was incomplete, and there were few bristles on the body and no legs on the thorax and abdomen (Fig. 5F). These phenotypes indicate that the early embryonic developmental process is severely disrupted by *Dnmt1*, *C/EBPg*, or *YBP* RNAi. These results also suggest that the interaction between C/EBPg and YBP has a greater effect on the expression of *Dnmt1*, participating in the development of silkworm embryos.

Highly expressed C/EBPg resulted in higher expression of *Dnmt1* in the *B. mori* ovary.

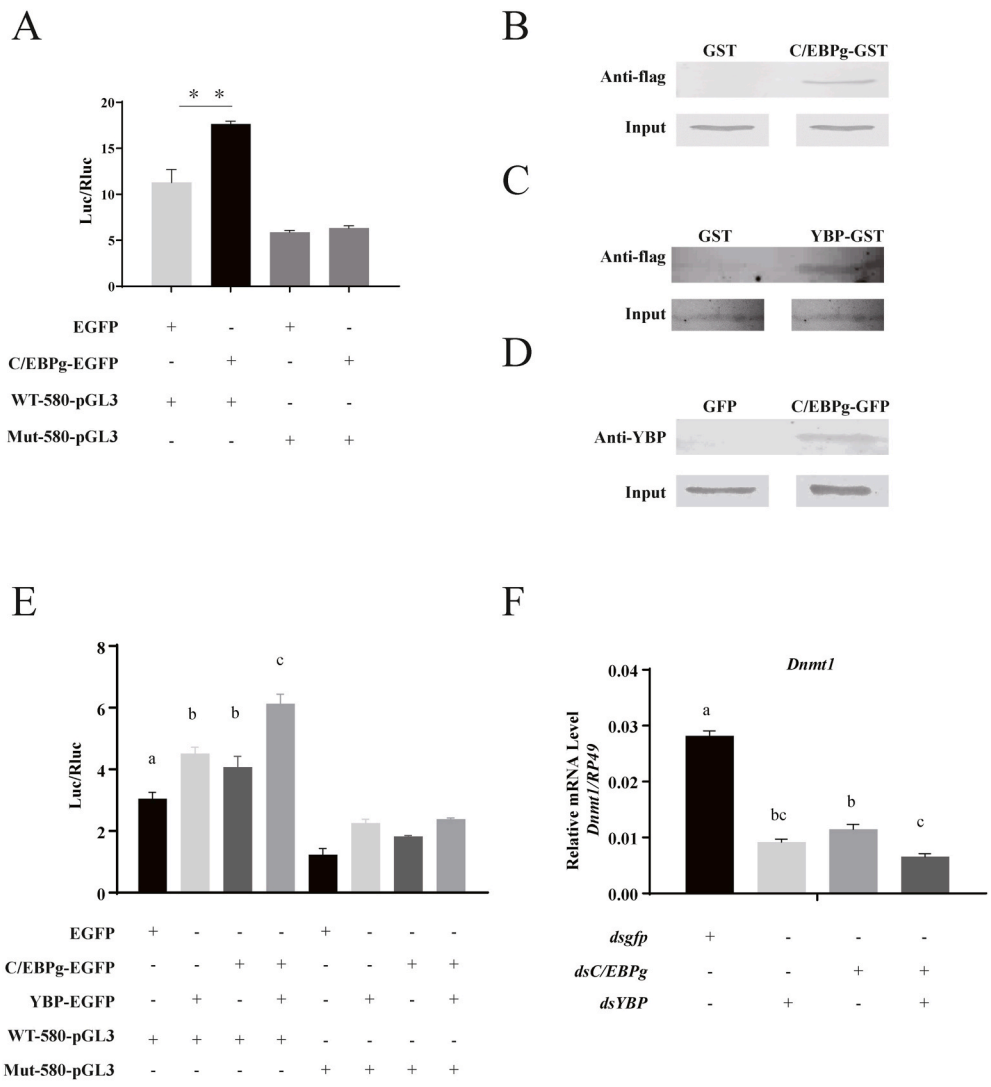

Fig. 4. The interaction of CCAAT/enhancer binding protein (C/EBPg) and YBP promotes *Dnmt1*expression. (A) The effect of C/EBPg overexpression in Bm12 cells to the luciferase activity of the −580to −560 region. EGFP was used as a control. (B to C) The interaction between C/EBPg and YBP proteins by GST-pulldown. The C/EBPg-GST protein was used as a bait protein to verify the fishing to YBP (B), and reverse verification (C). Input as a loading control. (D) Co-ip experiment that C/EBPg-GFP bound to YBP in Bm12 cells. (E) The effect of overexpression of YBP or/and C/EBPg in Bm12 cells on the activity of the −580 to −560 region. (F) The effect of knocking down of *YBP* or/and *C/EBPg* in Bm12 cells on the mRNA level of *Dnmt1*. The relative mRNA level of *Dnmt1* was normalized to the expression level of *RP49*. Each data point is the mean ± SEM of three independent assays. For the *t*-test: *p < 0.05, **p < 0.01, ***p < 0.001.

Besides regulation of hatch rate, *Dnmt1* has been reported to regulate ovarian development (Bewick et al., 2019). *Dnmt1* was highly expressed in the early developmental stages of *B. mori* embryos (Fig. 1A), implying that *Dnmt1* function in embryos may be similar to the maternal parent. Does the interaction of C/EBPg and YBP regulate *Dnmt1* expression in the *B. mori* ovary as in the embryo? The expression of *Dnmt1* in different tissues in one-day-old pupae was determined. The result showed that *Dnmt1* was highly expressed in the ovary and testis, and the mRNA level of *Dnmt1* in the ovary was much higher than in the testis (Fig. 6A); *YBP* was expressed in the ovary and testis, but there was no difference in the mRNA or protein expression levels of *YBP* between the two tissues (Fig. 6B and D); *C/EBPg* was significantly expressed in the ovary at mRNA and protein levels (Fig. 6C and D). The expression profiles of these genes suggest that C/EBPg and YBP may enhance *Dnmt1* expression in the *B. mori* ovary, and C/EBPg may be the factor regulating higher *Dnmt1* expression in the ovary. (See Fig. 7)

4. Discussion

Dnmt1 plays an important role in insect embryonic development, and *Dnmt1* RNAi resulted in a decrease in the egg hatch rate of *B. mori* (Xiang et al., 2013). In this study, we showed that transcription factors C/EBPg and YBP formed a complex to enhance *Dnmt1* transcription. Knockdown of *C/EBP* or *YBP* decreased the hatch rate, and simultaneous RNAi of both genes resulted in hatching failure as *Dnmt1* RNAi did (Fig. 5E). Thus, we demonstrated that the interaction of C/EBP and YBP regulates *Dnmt1* expression and subsequent embryonic development. Our results showed that *Dnmt1* and *YBP* were upregulated 12–14 h after fertilization (before the organogenesis stage), while *C/EBP* was expressed almost throughout the entire first day of embryonic development (Fig. 5A and B), suggesting that *C/EBP* regulates the expression of other genes besides *Dnmt1*. This may be the reason why *C/EBP* RNAi affects hatch rate more than *YBP* RNAi (Fig. 5E). Besides, the expression of *Dnmt1*, *C/EBP*, and *YBP* during early embryonic development (Fig. 5A and B) and the phenotypes of RNAi of these genes (Fig. 5F) suggest that DNA methylation affects early embryonic development. However, how *Dnmt1*, *YBP*, and *C/EBP* are upregulated at the early stages and how they affect *B. mori* embryonic development requires further investigation.

The expression levels of Dnmt1 are related to the DNA methylation rate and function in insect development. By analyzing *Dnmt1* expression levels in the different tissues of pupae, we demonstrated that *Dnmt1* was highly expressed in the sex glands, and the expressional level of *Dnmt1* in the ovary was higher than in the testis (Fig. 6A). We found that transcription factor YBP was highly expressed in the ovary and testis, and this may be the reason why *Dnmt1* was expressed in the sex glands more than in other tissues (Fig. 6B). We also found that C/EBP was highly expressed in the ovary, resulting in higher expression of *Dnmt1* in the ovary than in the testis. However, how Dnmt1 expressional levels or DNA methylation rates in different tissues are related to DNA methylation function remains unclear. A higher DNA methylation rate or more

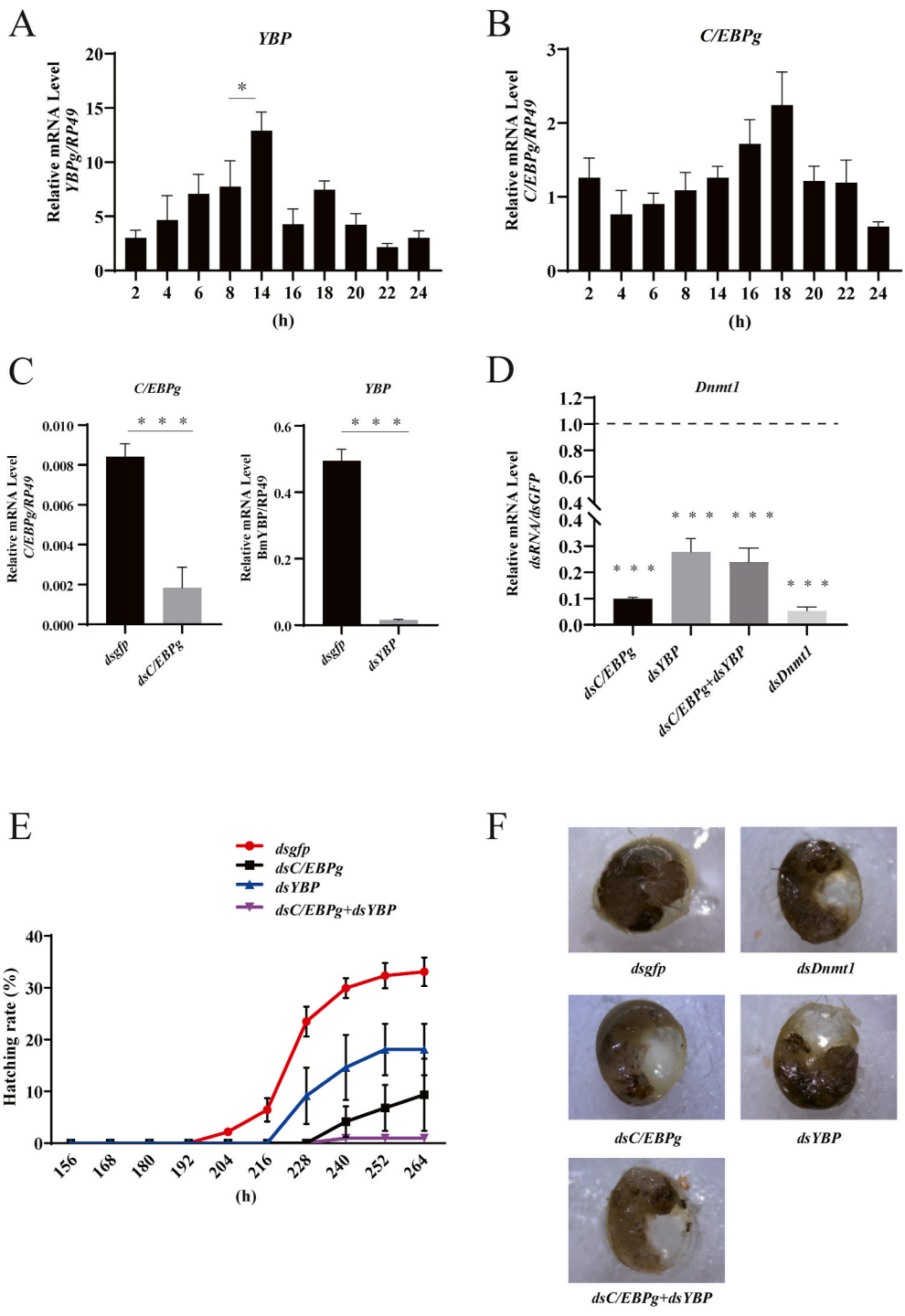

Fig. 5. C/EBPg and YBP participate in the hatch process of *B. mori* fertilized eggs by coordinately regulating *Dnmt1* expression. (A to B) *YBP* (A) and *C/EBPg* (B) expression profiles on the first day of *B. mori* embryonic development. The relative mRNA level of *Dnmt1* was normalized to the expression level of *RP49*. (C) The mRNA levels of *C/EBPg* (left) and *YBP* (right) 24 h post *C/EBPg* or *YBP* dsRNA was injected into newly fertilized eggs. (D) The mRNA levels of *Dnmt1* 24 h post *C/EBPg* or/and dsRNAs were injected into newly fertilized eggs. (E) The hatch rates of *C/EBPg* or/and *YBP* dsRNA-injected fertilized eggs. (F) The phenotypes of *Dnmt1*, *C/EBPg*, or/and *YBP* dsRNA-injected fertilized eggs at 180 h after egg deposition. Each data point is the mean ± SEM of three independent assays. For the *t*-test: *p < 0.05, **p < 0.01, ***p < 0.001.

methylated genes may be required for ovarian development. While in the pupal wing disc, the expressional level of *Dnmt1* is very low compared to that in other tissues (Fig. 6A), but DNA methylation plays a role in wing development by inhibiting the expression of transcription factor *ara* mediated-chitinase (Xu et al., 2020). Therefore, different Dnmt1 expression levels meet the developmental needs of different tissues.

DNA methylation regulates tissue-specific gene expression. However, how *Dnmt* is expressed in special tissues is unclear. In this study, we found that gonad-specific YBP activated *Dnmt1* expression in the ovary, testis, and fertilized egg. By pull-down and Co-ip experiments, we demonstrated that YBP and C/EBPg bound each other to form a complex to activate *Dnmt1* expression (Fig. 4). These results suggest that the formation of YBP, C/EBPg, and DNA complex significantly enhances *Dnmt1* expression. BmC/EBPg was highly expressed in the ovary and the embryo (Fig. 6C), and this may explain why *Dnmt* is expressed at a higher level in these tissues than in other tissues. Interestingly, YB1 has been reported to down-regulate the expression of carbamoyl phosphate synthetase-I (CPS1) by inhibiting the function of C/EBPa. YB1 can be recruited to the proximal promoter of CSP1, thereby inhibiting the upregulation of CPS1 expression induced by the transcription factor C/EBPa on the same proximal promoter (Chen et al., 2009). However, the regulation of *Dnmt1* in this study was different from the inhibition of C/EBPa-mediated CPS1 expression by YB1. YBP can interact with

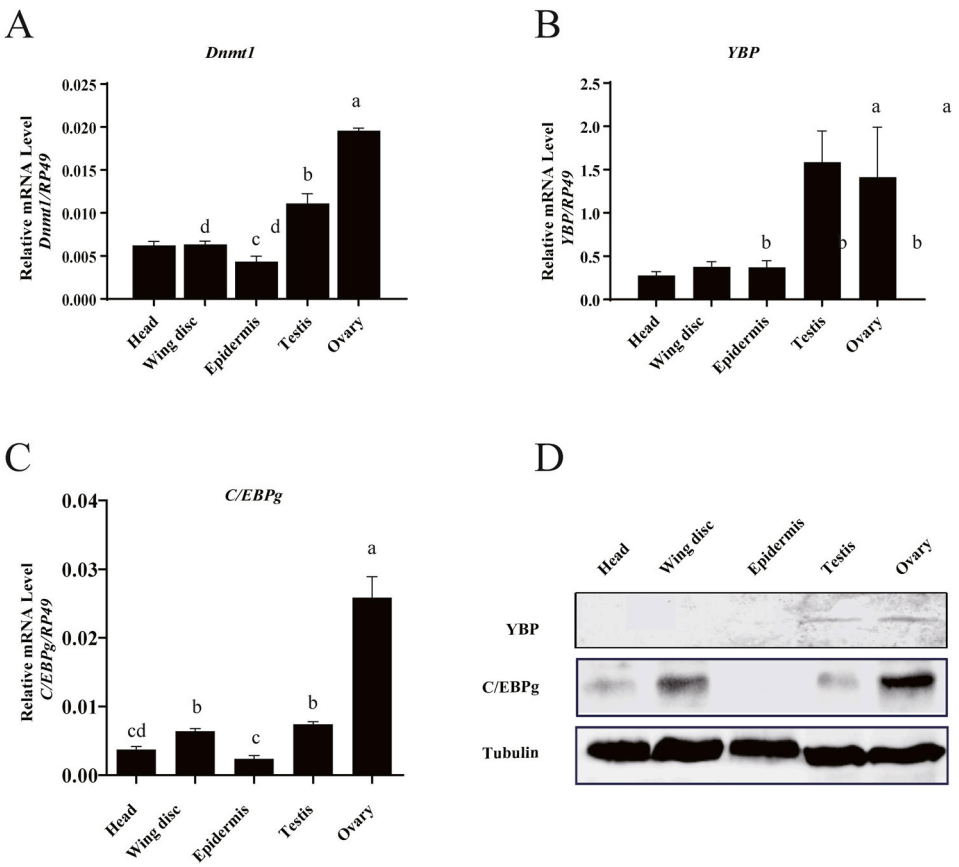

Fig. 6. The expression analysis of *Dnmt1*, *YBP*, and *C/EBPg* in different tissues of one-day-old pupa. (A to C) The mRNA levels of *Dnmt1* (A), *YBP* (B), and *C/EBPg* (C) in various tissues were detected by qPCR. The relative mRNA level was normalized to the expression level of *18S* rRNA. (D) Protein levels of YBP and C/EBPg in various tissues were detected by Western bolt. Each data point is the mean ± SEM of three independent assays. For the *t*-test: *p < 0.05, **p < 0.01, ***p < 0.001.

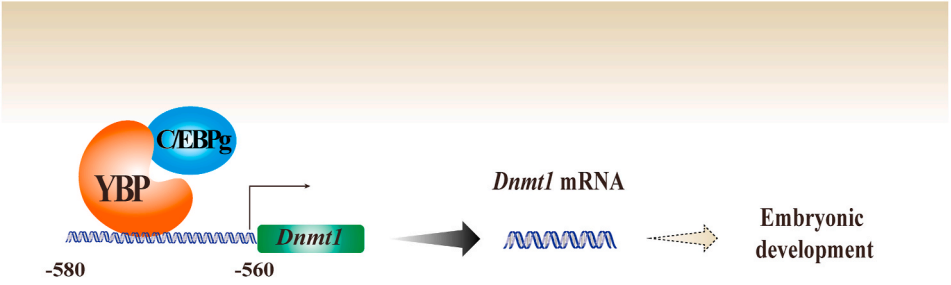

Fig. 7. The model of the regulation of *BmDmnt1*expression in *B. mori* embryonic stage.

C/EBPg to promote the expression of *Dnmt1*. Besides C/EBPg and YBP, it is possible that there may be other regulatory pathways that enhance *Dnmt1* expression, since the double knockdown of *C/EBPg* and *YBP* did not completely inhibit *Dnmt1* expression (Fig. 5D). However, the effect of double knockdown of *C/EBPg* and *YBP* on the hatchability (Fig. 5E) was similar to *Dnmt1* RNAi (Fig. 1B), suggesting that C/EBPg or YBP regulates multi-gene expression besides *Dnmt1*. For example, C/EBPg activates the expression of *B. mori* CREB-binding protein (Lyu et al., 2020), which is important for insect development (Atkins et al., 2016; Francis et al., 2016). These results indicate that C/EBPg is an important regulator of insect development.

YB1 is a multifunctional protein involved in a variety of cellular processes and human malignant tumors, such as malignant melanoma (Kosnopfel et al., 2014), ovarian cancer (Panupinthu et al., 2014), and Alzheimer's Disease (Bobkova et al., 2015). It is therefore considered to be a target gene for tumor treatment. In addition, YB1 has also been reported to be related to mouse ovarian development. The phosphorylation of YB1 during stages of follicle maturation to ovulation is required for follicle-stimulating hormone (FSH)-mediated target gene expression (Donaubauer and Hunzicker-Dunn, 2016). In *D. melanogaster*, the YBX1 homolog, YPS, promotes the development of ovarian germ line stem cells by preferentially recognizing 5-methylcytosine RNAs (Zou et al., 2020). In this study, we showed that YBP is expressed in the *B. mori* ovary, testis, and fertilized eggs, indicating its involvement in regulation of *B. mori* reproduction.

In summary, this study reveals a regulatory mechanism of *Dnmt1* expression in reproductive organs. YBP regulates the expression of *Dnmt1* to affect gonad development, while the ovarian and embryo-specific transcription factor C/EBPg interacts with YBP to enhance *Dnmt1* expression. Reproduction-related YBP and C/EBPg enhance *Dnmt1* expression, leading to the development of the ovary and embryos.

Acknowledgments

This work was supported by the National Natural Science Foundation of China (No. 31872286).

Appendix A. Supplementary data

Supplementary data to this article can be found online at https://doi.org/10.1016/j.ibmb.2021.103583.

Credit author statement

Hao Lyu: Methodology, Investigation, Data Curation, Writing - Original Draft, Guanfeng Xu: Resources, Xuezhen Peng & Chengcheng Gong: Resources, Yuling Peng: Resources, Qisheng Song & Qili Feng: Review, Sichun Zheng: Conceptualization, Supervision, Project administration, Writing- Reviewing and Editing, Funding acquisition

References

Atkins, M., Potier, D., Romanelli, L., Jacobs, J., Mach, J., Hamaratoglu, F., Aerts, S., Halder, G., 2016. An ectopic network of transcription factors regulated by hippo signaling drives growth and invasion of a malignant tumor model. Curr. Biol. 26, 2101–2113.

Bewick, A.J., Sanchez, Z., McKinney, E.C., Moore, A.J., Moore, P.J., Schmitz, R.J., 2019. Dnmt1 is essential for egg production and embryo viability in the large milkweed bug, Oncopeltus fasciatus. Epigenet. Chromatin 12, 6.

Bird, A., 2002. DNA methylation patterns and epigenetic memory. Genes Dev. 16, 6–21.

Bobkova, N.V., Lyabin, D.N., Medvinskaya, N.I., Samokhin, A.N., Nekrasov, P.V., Nesterova, I.V., Aleksandrova, I.Y., Tatarnikova, O.G., Bobylev, A.G., Vikhlyantsev, I.M., Kukharsky, M.S., Ustyugov, A.A., Polyakov, D.N., Eliseeva, I.A., Kretov, D.A., Guryanov, S.G., Ovchinnikov, L.P., 2015. The Y-box binding protein 1 suppresses alzheimer's Disease progression in two animal models. PloS One 10, e0138867.

Bonasio, R., Tu, S., Reinberg, D., 2010. Molecular signals of epigenetic states. Science 330, 612–616.

Cedar, H., Bergman, Y., 2009. Linking DNA methylation and histone modification: patterns and paradigms. Nat. Rev. Genet. 10, 295–304.

Chen, Y.R., Sekine, K., Nakamura, K., Yanai, H., Tanaka, M., Miyajima, A., 2009. Y-box binding protein-1 down-regulates expression of carbamoyl phosphate synthetase-I by suppressing CCAAT enhancer-binding protein-alpha function in mice. Gastroenterology 137, 330–340.

Donaubauer, E.M., Hunzicker-Dunn, M.E., 2016. Extracellular signal-regulated kinase (ERK)-dependent phosphorylation of Y-Box-binding protein 1 (YB-1) enhances gene expression in granulosa cells in response to follicle-stimulating hormone (FSH). J. Biol. Chem. 291, 12145–12160.

Feng, S., Cokus, S.J., Zhang, X., Chen, P.Y., Bostick, M., Goll, M.G., Hetzel, J., Jain, J., Strauss, S.H., Halpern, M.E., Ukomadu, C., Sadler, K.C., Pradhan, S., Pellegrini, M., Jacobsen, S.E., 2010. Conservation and divergence of methylation patterning in plants and animals. Proc. Natl. Acad. Sci. U. S. A. 107, 8689–8694.

Francis, M.J., Roche, S., Cho, M.J., Beall, E., Min, B., Panganiban, R.P., Rio, D.C., 2016. Drosophila IRBP bZIP heterodimer binds P-element DNA and affects hybrid dysgenesis. Proc. Natl. Acad. Sci. U. S. A. 113, 13003–13008.

Goll, M.G., Kirpekar, F., Maggert, K.A., Yoder, J.A., Hsieh, C.L., Zhang, X., Golic, K.G., Jacobsen, S.E., Bestor, T.H., 2006. Methylation of tRNAAsp by the DNA methyltransferase homolog Dnmt2. Science 311, 395–398.

Hackett, J.A., Reddington, J.P., Nestor, C.E., Dunican, D.S., Branco, M.R., Reichmann, J., Reik, W., Surani, M.A., Adams, I.R., Meehan, R.R., 2012. Promoter DNA methylation couples genome-defence mechanisms to epigenetic reprogramming in the mouse germline. Development 139, 3623–3632.

Jaenisch, R., Bird, A., 2003. Epigenetic regulation of gene expression: how the genome integrates intrinsic and environmental signals. Nat. Genet. 33 (Suppl. l), 245–254.

Kay, S., Skowronski, D., Hunt, B.G., 2018. Developmental DNA methyltransferase expression in the fire ant Solenopsis invicta. Insect Sci. 25, 57–65.

Khurad, A.M., Zhang, M.J., Deshmukh, C.G., Bahekar, R.S., Tiple, A.D., Zhang, C.X., 2009. A new continuous cell line from larval ovaries of silkworm, Bombyx mori. In Vitro Cell. Dev. Biol. Anim. 45, 414–419.

Kosnopfel, C., Sinnberg, T., Schittek, B., 2014. Y-box binding protein 1–a prognostic marker and target in tumour therapy. Eur. J. Cell Biol. 93, 61–70.

Kostal, V., Simunkova, P., Kobelkova, A., Shimada, K., 2009. Cell cycle arrest as a hallmark of insect diapause: changes in gene transcription during diapause induction in the drosophilid fly, Chymomyza costata. Insect Biochem. Mol. Biol. 39, 875–883.

Livak, K.J., Schmittgen, T.D., 2001. Analysis of relative gene expression data using real-time quantitative PCR and the 2(-Delta Delta C(T)) Method. Methods 25, 402–408.

Lyko, F., Maleszka, R., 2011. Insects as innovative models for functional studies of DNA methylation. Trends Genet. 27, 127–131.

Lyu, H., Xu, G., Chen, P., Song, Q., Feng, Q., Yi, Y., Zheng, S., 2020. 20-Hydroxyecdysone receptor-activated Bombyx mori CCAAT/enhancer-binding protein gamma regulates the expression of BmCBP and subsequent histone H3 lysine 27 acetylation in Bo. mori. Insect Mol. Biol. 29, 256–270.

Mitsudome, T., Mon, H., Xu, J., Li, Z., Lee, J.M., Patil, A.A., Masuda, A., Iiyama, K., Morokuma, D., Kusakabe, T., 2015. Biochemical characterization of maintenance DNA methyltransferase DNMT-1 from silkworm, Bombyx mori. Insect Biochem. Mol. Biol. 58, 55–65.

Panupinthu, N., Yu, S., Zhang, D., Zhang, F., Gagea, M., Lu, Y., Grandis, J.R., Dunn, S.E., Lee, H.Y., Mills, G.B., 2014. Self-reinforcing loop of amphiregulin and Y-box binding protein-1 contributes to poor outcomes in ovarian cancer. Oncogene 33, 2846–2856.

Robinson, K.L., Tohidi-Esfahani, D., Ponton, F., Simpson, S.J., Sword, G.A., Lo, N., 2016. Alternative migratory locust phenotypes are associated with differences in the expression of genes encoding the methylation machinery. Insect Mol. Biol. 25, 105–115.

Sengupta, S., Mantha, A.K., Mitra, S., Bhakat, K.K., 2011. Human AP endonuclease (APE1/Ref-1) and its acetylation regulate YB-1-p300 recruitment and RNA polymerase II loading in the drug-induced activation of multidrug resistance gene MDR1. Oncogene 30, 482–493.

Shao, X.L., He, S.Y., Zhuang, X.Y., Fan, Y., Li, Y.H., Yao, Y.G., 2014. mRNA expression and DNA methylation in three key genes involved in caste differentiation in female honeybees (Apis mellifera). Dongwuxue Yanjiu 35, 92–98.

Sourmeli, S., Papantonis, A., Lecanidou, R., 2005. BmCbZ, an insect-specific factor featuring a composite DNA-binding domain, interacts with BmC/EBPgamma. Biochem. Biophys. Res. Commun. 338, 1957–1965.

Ventos-Alfonso, A., Ylla, G., Montanes, J.C., Belles, X., 2020. DNMT1 promotes genome methylation and early embryo development in cockroaches. iScience 23, 101778.

Xiang, H., Li, X., Dai, F., Xu, X., Tan, A., Chen, L., Zhang, G., Ding, Y., Li, Q., Lian, J., Willden, A., Guo, Q., Xia, Q., Wang, J., Wang, W., 2013. Comparative methylomics between domesticated and wild silkworms implies possible epigenetic influences on silkworm domestication. BMC Genom. 14, 646.

Xiang, H., Zhu, J., Chen, Q., Dai, F., Li, X., Li, M., Zhang, H., Zhang, G., Li, D., Dong, Y., Zhao, L., Lin, Y., Cheng, D., Yu, J., Sun, J., Zhou, X., Ma, K., He, Y., Zhao, Y., Guo, S., Ye, M., Guo, G., Li, Y., Li, R., Zhang, X., Ma, L., Kristiansen, K., Guo, Q., Jiang, J., Beck, S., Xia, Q., Wang, W., Wang, J., 2010. Single base-resolution methylome of the silkworm reveals a sparse epigenomic map. Nat. Biotechnol. 28, 516–520.

Xu, G., Yi, Y., Lyu, H., Gong, C., Feng, Q., Song, Q., Peng, X., Liu, L., Zheng, S., 2020. DNA methylation suppresses chitin degradation and promotes the wing development by inhibiting Bmara-mediated chitinase expression in the silkworm, Bombyx mori. Epigenet. Chromatin 13, 34.

Xu, G., Zhang, J., Lyu, H., Song, Q., Feng, Q., Xiang, H., Zheng, S., 2018. DNA methylation mediates BmDeaf1-regulated tissue- and stage-specific expression of BmCHSA-2b in the silkworm, Bombyx mori. Epigenet. Chromatin 11, 32.

Yan, H., Bonasio, R., Simola, D.F., Liebig, J., Berger, S.L., Reinberg, D., 2015. DNA methylation in social insects: how epigenetics can control behavior and longevity. Annu. Rev. Entomol. 60, 435–452.

Yang, S.X., Guo, C., Xu, M., Sun, J.T., Hong, X.Y., 2014. Sex-dependent activity of de novo methyltransferase 3 (Tudnmt3) in the two-spotted mite, Tetranychus urticae Koch. Insect Mol. Biol. 23, 743–753.

Zhang, J., Xing, Y., Li, Y., Yin, C., Ge, C., Li, F., 2015. DNA methyltransferases have an essential role in female fecundity in brown planthopper, Nilaparvata lugens. Biochem. Biophys. Res. Commun. 464, 83–88.

Zhou, X., Chen, J., Liang, M.S., Wang, F., 2013. Differential DNA methylation between two wing phenotypes adults of Sogatella furcifera. Genesis 51, 819–826.

Zou, F., Tu, R., Duan, B., Yang, Z., Ping, Z., Song, X., Chen, S., Price, A., Li, H., Scott, A., Perera, A., Li, S., Xie, T., 2020. Drosophila YBX1 homolog YPS promotes ovarian germ line stem cell development by preferentially recognizing 5-methylcytosine RNAs. Proc. Natl. Acad. Sci. U. S. A. 117, 3603–3609.

Zwier, M.V., Verhulst, E.C., Zwahlen, R.D., Beukeboom, L.W., van de Zande, L., 2012. DNA methylation plays a crucial role during early Nasonia development. Insect Mol. Biol. 21, 129–138.